International Journal of Minerals, Metallurgy and Materials
Accepted manuscript, https://doi.org/10.1007/s12613-019-1933-3
© University of Science and Technology Beijing and Springer-Verlag GmbH Germany, part of Springer Nature 2019

Effects of chelating agent on sol-gel synthesis of nano zirconia: The comparison of Pechini and sugar-based methods

Faramarz Kazemi [a], Farzin Arianpour [b], Mahdiar Taheri [c], Ali Saberi [d], and Hamid Reza Rezaie [e,]*

[a] Department of Mining and Metallurgy, Amirkabir University of Technology, Tehran, Iran.

[b] Research and Application Center, Kastamonu University, Kastamonu, Turkey.

[c] College of Engineering and Computer Science, The Australian National University, Canberra, Australia.

[d] Materials Processing, Faculty of Engineering Science, University of Bayreuth, Bayreuth, Germany.

[e] School of Metallurgy and Materials Engineering, Iran University of Science and Technology, Tehran, Iran.

[*] Corresponding author: hrezaie@iust.ac.ir (H.R. Rezaie).

Abstract: This study reports on the comparison of the Pechini and sugar-based combustion synthesis to produce nano zirconia. It involves utilizing zirconium hydroxide as a metal precursor and citric acid, sucrose and fructose as chelating agents, followed by calcination at 500, 600, and 700 °C in air. The characterizations were thermal analysis, specific surface area, Fourier transform infra-red spectroscopy, X-ray diffraction, scanning, and transmission electron microscopy. The highest specific surface area (27 $m^2 g^{-1}$) and smallest particle size (39.1 nm) were obtained for fructose at 700 °C. The X-ray study revealed the formation of the single phase tetragonal zirconia via fructose after calcination at 500 °C, while for sucrose and citric acid, mixtures of monoclinic and tetragonal phases were obtained. The tetragonality parameter was determined using diffraction data and proved it increases with increasing the temperature. The presence and formation mechanism of the stabilized tetragonal zirconia were also discussed based on the X-ray and electron diffraction studies.

Keywords: Zirconia; Nano powder; Sol-gel; Sugar; Pechini; Chelation

1. Introduction

Wet chemical method based on the hydroxides precipitation from salts or alkoxides hydrolysis, is a kind of effective routes to produce oxides nano powders [1]. Among them, sugar-based acid catalyzed sol-gel is known as a common technique for ceramic nano powders [2]. In this route, different sugars (e.g., sucrose, maltose, fructose, or glucose) are generally used as seeding templates to synthesize nano oxides with tailored pore size [3]. Sugar acts as a chelating agent to homogenously keep ions in the solution by a process involves dehydration of metal complexes, followed by the sugar decomposition [2,4].

Accepted Manuscript. Not Copyedited

After dehydration, a dark gel is obtained and by heat-treating in air, a nano powder is produced. In this case, the degree of porosity has a direct relation to the amounts of gases that generate during process [2-5]. Pechini (citrate-based) route is developed to avoid some disadvantages of conventional methods such as in-homogeneity [6]. The aim of this technique is to obtain a uniform mixture based on the metal cations chelating using a hydroxyl carboxylic acid, e.g., citric acid [6,7]. By a followed heat-treatment after chelation, the mixture transforms to a gel, the excess water is removed and poly-esterification happens [7]. The polymeric gel is finally calcined at relatively high temperatures to remove all residue organic matters [6-9]. The preparation of nano zirconia was reported using sucrose [10,11], maltose [12], glucose/fructose [13] and citric acid [14-17]. A brief overview on some recent researches is presented in Table 1. In this Table, c refers to cubic zirconia, t represents tetragonal zirconia, *T* is temperature and *CS* is crystallite size.

Table 1. Nano tetragonal zirconia synthesis via sugar-based and Pechini methods.

Precursor	Chelating agent	*T* / °C	Phase	*CS* / nm	Ref.
Oxy-chloride	Sucrose	600	c	6-10	[10]
Acetylacetonate	Sucrose	490	t	12.7-33.5	[11]
Nitrate	Maltose	500	t	---	[12]
Iso-propoxide	Glucose/Fructose	700	t, m	16-23	[13]
Oxy-nitrate	Citric acid	600	t	9	[14]
Oxy-chloride	Citric acid	700	t	10.2-32.9	[15]
Oxy-nitrate	Citric acid	625	t, c	12.5-14.8	[16]
Acetylacetonate	Citric acid	490	t	13.4	[17]

Several zirconium sources (e.g., nitrate [12,18], oxy-nitrate [15,19], chloride [3,20] oxy-chloride [10,16,21], iso-propoxide [20,22-24], n-butoxide [13], and acetylacetonate [14,17]) have been tried for the synthesis of nano zirconia. Most of these compounds are generally cost-expensive, flammable/explosive, toxic and potentially harmful for human or environment. In this work, zirconium hydroxide ($Zr(OH)_4$) was used as a precursor as well as citric acid, sucrose and fructose as chelating agents to synthesize nano tetragonal zirconia at low temperatures. These chelating agents are expected as kinds of green materials which are not dangerous. The effects of them are investigated on the gel formation, thermal decomposition and nano powder characteristics by thermal analysis (DTA/TG), Fourier transform infra-red spectroscopy (FT-IR), specific surface area measurement, X-ray diffraction (XRD), and scanning and transmission electron microscopy (FE-SEM/TEM).

2. Experimental

2.1. Materials

Accepted Manuscript Not Copyedited

Zirconium hydroxide ($Zr(OH)_4$) was used as zirconium precursor. This powder was previously synthesized via a facile, green and economical roast-leach method from commercially available zircon sand [25]. It has a chemical purity of >99.5 wt.% and is easily soluble in nitric acid. Chemically-graded sucrose, fructose and citric acid were selected as chelating agents. The other used chemicals were nitric acid (65 wt.%), ammonia solution (25 wt.%) and polyvinyl alcohol (PVA, molecular weight = 160,000 g mol^{-1}). All purchased chemicals were used as-received without any further purification. The characteristics of the used chemicals are listed in Table 2.

Table 2. Characteristics of the used chemical materials.

Material	Formula	Function	Cat. No.	Supplier
Zirconium hydroxide	$Zr(OH)_4$	Precursor	---	---
Sucrose	$C_{12}H_{22}O_{11}$	Chelating agent	S9378	Sigma-Aldrich, USA
Fructose	$C_6H_{12}O_6$	Chelating agent	239704	Sigma-Aldrich, USA
Citric acid	$C_6H_8O_7{\cdot}H_2O$	Chelating agent	100247	Merck, Germany
Nitric acid	HNO_3	Solvent	100441	Merck, Germany
Ammonia	NH_4OH	pH adjustment	105432	Merck, Germany
Polyvinyl alcohol	$(C_2H_4O)_x$	Polymerization agent	363065	Sigma-Aldrich, USA

2.2. Synthesis

In the Pechini method, the molar ratio of citric acid to zirconium hydroxide was adjusted to 0.5:1. The zirconium hydroxide was dissolved into nitric acid and then citric acid was added during mixing at 80 °C for 2 h. Citric acid acts as a chelating agent (to bind zirconium ions and prohibit precipitation during pH variations) and also a fuel to promote reactions. The pH of the solution was adjusted to 6 by drop-wise addition of ammonium hydroxide solution. The mixture was again stirred at 120 °C for 4 h and then dried in an electric oven at 180 °C for 4 h to transform to a gel. In the sugar-based method, the stoichiometric mole ratio of zirconium hydroxide, sugars and PVA was adjusted to 1:4:0.5 for sucrose and 1:8:0.5 for fructose. Sols were prepared by dissolving zirconium hydroxide and PVA in nitric acid, addition of sucrose/fructose to the solutions and then mixing at 80 °C for 2 h. The pH was adjusted to 1 by drop-wise addition of diluted nitric acid and mixing continued for additionally 4 h. The sols were then dried at 200 °C for 4 h in the oven. All prepared gels were gently powdered and micronized using an agate mill and passed through a 325 mesh (44 µm) sieve to produce homogenous powders and break large agglomerates. Samples were then poured into alumina crucibles and calcined at 500, 600 and 700 °C for 1 h soaking time in an electric furnace in air. The calcination temperatures were selected according to the thermal analysis results. The flowcharts of the Pechini and sugar-based methods are shown in Figs. 1(A) and (B).

Accepted Manuscript Not Copyedited

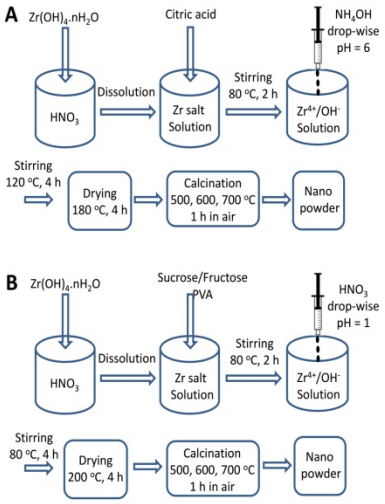

Fig. 1. Nano zirconia synthesis via: (A) Pechini and (B) sugar-based methods.

2.3. Characterization

Differential thermal analysis (DTA) and thermo-gravimetric (TG) tests were carried out on a 449-C thermal analyzer (Netzsch, Germany) using alumina cell, heating rate of 10 °C min^{-1} up to 750 °C in air. Fourier transform infra-red (FT-IR) spectra were recorded in the range of 4000-400 cm^{-1} using an IR spectrometer (Shimadzu, Japan). Pellets were prepared by pressing a mixture of spectral grade KBr and 1 wt.% of samples. Raman Spectroscopy was performed at room temperature using a LabRam system (Horiba, Japan). The samples were excited with a 532 nm laser, and the spectrum was obtained via a silicon charge coupled device (CCD) detector. Phase composition was monitored by X-ray diffractometery (XRD) on an AXS-2002 diffractometer (Bruker, USA) using Ni-filtered Cu $K_{\alpha 1}$ radiation (λ=0.15406 nm) in the 2θ range of 10-70°, step size 0.02°, time per step 1 s and generator setting of 40 kV, 40 mA at room temperature. The apparent crystallite sizes were measured according to the Scherrer equation (Eq. (1)) [26]. In this formula, λ is the X-ray wavelength, θ_0 is the Bragg angle, k is a constant (0.9) and L is the apparent crystallite size in nm. $\beta(2\theta)$ (in radians) is the peak full-width at half maximum intensity (FWHM) was taken as the experimental full-width (β_{exp}) and corrected for the experimental broadening (β_{ins}) according to Eq. (2) [27]. The β_{ins} parameter was measured experimentally using silicon. The volume fractions of monoclinic (V_m) and tetragonal (V_t) phases were determined according to the Eqs. (3) and (4) [14,28,29]. In the Eq. (4), parameter I indicates the X-ray peak intensity of the mentioned crystalline page. Eq. (5) was used for lattice parameters' calculation of tetragonal zirconia phase [26]. In this equation h, k and l are crystalline plane indices, a and c are tetragonal crystal lattices (in Å) and d is the crystalline page distance (in Å).

$$\beta(2\theta) = \frac{k\ \lambda}{L\cos(\theta_0)} \quad (1)$$

Accepted Manuscript Not Copyedited

$$\beta(2\theta) = \left(\beta^2_{exp} - \beta^2_{ins}\right)^{1/2} \quad (2)$$

$$V_t = \frac{1.311?X_m}{1+\quad X_m} ?\mathbb{V} = ?\ 0 - ?V_m \quad (3)$$

$$X_m = \frac{I_m ?(\bar{1}11) + I_m(\quad)\quad \#}{I_m ?(\bar{1}11) + I_m(\quad) + I_t(\quad)} \quad (4)$$

$$\frac{1}{d^2} = \frac{h^2+k^2}{a^2} + \frac{l^2}{c^2} \quad (5)$$

Specific surface area was measured according to the N_2-physisorption and Brunauer-Emmett-Teller (BET) method at 77 K on a Gemini ASAP-2010 (Micromeritics, USA) system using ultra-pure nitrogen gas. To remove the absorbents, samples were degassed at 100 °C for 2 h under vacuum before the test. Particle sizes (*d* nm) were derived from Eq. (6), where $\tilde{n}$ is the theoretical density of zirconia (5.68 g cm^{-3}) and *S* refers to the specific surface area of the samples in m^2 g^{-1} [30].

$$d = \frac{6000}{\tilde{n}?S} \quad (6)$$

Microstructural and morphological features were observed using a LEO-1530 field emission scanning electron microscope (Gemini FEG FE-SEM, Zeiss, Germany). To prepare the samples, powders were ultrasonically dispersed into isopropanol and a drop of suspension was spread on an aluminum plate by a syringe. Samples were then sputter coated with a thin gold-platinum layer to prevent from electron charge. A LIBRA 200 transmission electron microscope (TEM, Zeiss, Germany) with a 200 kV accelerating voltage was utilized for furthered high resolution imaging and electron diffraction. A diluted sol was prepared by ultrasound dispersion of powders into isopropanol, spreading a small drop on a 200 mesh copper grid, drying and then covering by an amorphous carbon film.

3. Results and discussion

3.1. Thermal behavior

Figs. 2(A) and (B) represent the thermal analysis curves (DTA and TG) of the prepared gels via Pechini and sugar-based methods using citric acid, sucrose and fructose as chelating agents. According to the DTA curves in Fig. 2(A), there is a sharp exothermic peak at 233 °C for citric acid (citrate) gel which is related to the decomposition of ammonium nitrate formed during gel preparation via Pechini method [27]. The weight loss behavior of sucrose shows slightly different behavior comparing with other chelating agents and happens in one step. It might be attributed to the complex structural and molecular changes of chelating agents especially for sugar molecules such as oxidation changes of the functional groups by temperature increase [4,27]. It also shows that the combustion of citrate gel was fulfilled in the range of 200-650 °C. The

Accepted Manuscript Not Copyedited

enthalpies of the reactions (released heat) using different chelating agents were calculated by measuring the area of the related DTA curves based on the J g^{-1} of the sample. For the Pechini process, the enthalpy was equal to 20.26 J g^{-1}. As it is clear, most of the heat was released around 230 $^{\circ}$C which might affect and increase the final particle sizes of the synthesized nano powders. The combustions of sucrose and fructose gels were completed before 555 $^{\circ}$C with the enthalpy values of 19.91 and 14.71 J g^{-1}, respectively. As it is demonstrated in the TG curves of Fig. 2(B), the weight loss of all gels gradually starts at about 150 $^{\circ}$C; however, it stops for citrate gel at higher temperature (670 $^{\circ}$C) in comparison with the sugar-based gels (550 $^{\circ}$C). It is clear that the decomposition of sucrose led to 83.5 wt.% weight loss while this amount was around 71.1 and 82.1 wt.% for fructose and citrate gels, respectively. The mass losses during heating of the sugar-based gels are attributed to the decomposition of organic chelating agents (sucrose and fructose) and burning of polymeric matrix (polyvinyl alcohol) [10, 13].

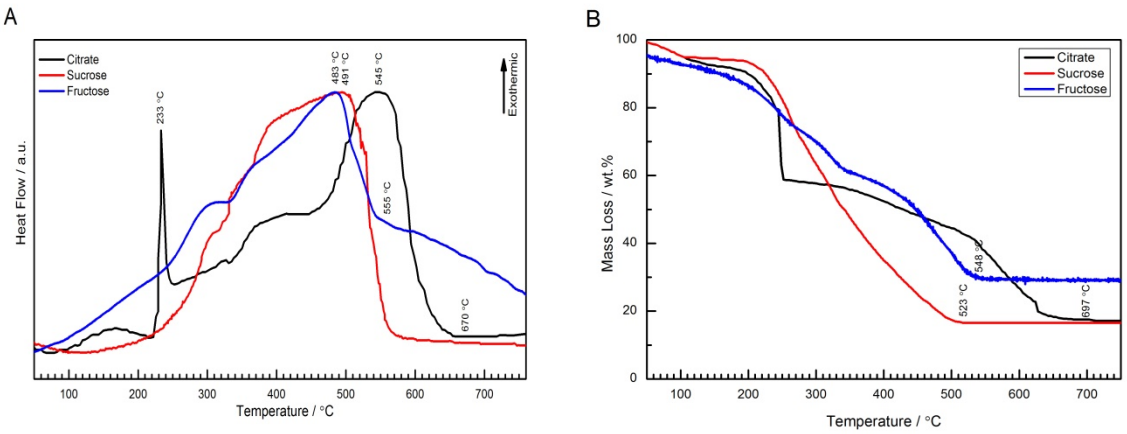

Fig. 2. Thermal analysis curves of the gels: (A) DTA and (B) TG.

In the sugar-based synthesis of nano zirconia, the released gases due to the decomposition of chelating agents produce a porous structure in the final powder [1]. The existing nitric acid in the starting sol leads to hydrolysis of sugar molecules and formation of primary fragments such as D-glucose or D-fructose. These basic sugar molecules have the same molar weight and chemical formula with different ring-type molecular structures. The decomposition energy of the sugar molecules is also enough to promote synthesis reaction, while, their free alcohol functions easily and homogenously trap metal cations in the finally produced gels [2-5]. Synthesized powders from wet chemical techniques are generally amorphous and easy to crystallize [6,7]. In the Pechini technique which is based on a citrate-nitrate reaction, metal ions are trapped in the homogeneous gel mixture which finally leads to the formation of molecular-scale nano oxide materials with a

Accepted Manuscript Copyedited

uniform composition [8]. Releasing the exothermic energy of metal-citrate complex, pushes forward the reaction and reduces the crystallization temperature of nano zirconia particles [6-9].

3.2. Phase characteristics

Fig. 3 shows the X-ray diffraction patterns of the synthesized nano zirconia powders using sucrose, fructose and citric acid as chelating agents and calcined at 500, 600 and 700 °C for 1 h in air. For the citrate sample calcined at 500 °C, the main phase composed of monoclinic zirconia. However, some small peaks related to the remained ammonium nitrate from Pechini process are also visible in the phase composition of this sample. It reveals that 500 °C in not enough temperature to fulfill the synthesis reaction in this process using citric acid as a chelating agent. By the way, this phase was disappeared by heating the gel at 600 and 700 °C. In the sucrose sample calcined at 500 °C, phase compositions consist of tetragonal and monoclinic zirconia mixtures, whereas for fructose one, XRD pattern just shows the presence of the tetragonal phase. After calcination at 600 °C, mixtures of tetragonal and monoclinic phases are visible for both citrate and sucrose samples. For fructose sample, tetragonal zirconia is still the unique phase in the mineral composition. This trend also continued after calcination of samples at 700 °C for 1 h. Table 3 shows the phase composition and diffraction data of the samples calcined at different temperatures. In this Table, *T* is calcination temperature, *V* is the phase volume fraction, *CS* is crystallite size, *FWHM* is full-width at half maximum of *2θ*, and t and m represent tetragonal and monoclinic phase of zirconia, respectively.

Accepted Manuscript Not Copyedited

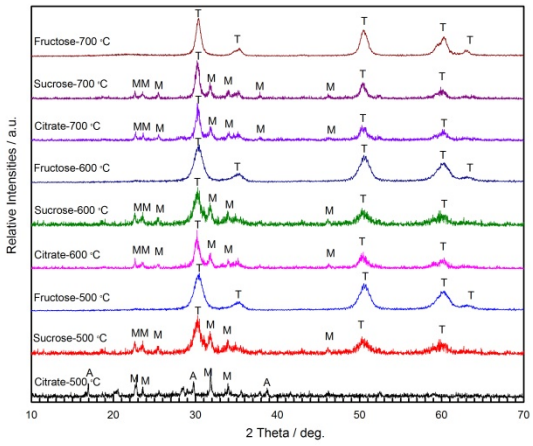

Fig. 3. X-ray diffraction patterns of the calcined powders.

Table 3. Phase composition and diffraction data.

Sample	*T* / °C	Phase	*V* / %	(*hkl*)	*2θ* / deg.	*FWHM*	*CS* / nm
Sucrose	500	t	66	(101)	30.273	0.820	9.2
		m	34	($\bar{1}$11)	31.760	0.396	20.8
Fructose		t	~100	(101)	30.478	1.170	7.02
Citrate		m	~100	($\bar{1}$11)	31.842	0.131	63.1
Sucrose	600	t	67	(101)	30.269	0.550	15.8
		m	33	($\bar{1}$11)	31.762	.360	22.9
Fructose		t	~100	(101)	30.382	0.650	12.6
Citrate		t	71	(101)	30.180	0.491	16.8
		m	29	($\bar{1}$11)	31.842	0.389	21.5
Sucrose	700	t	74	(101)	30.243	0.520	15.9
		m	26	($\bar{1}$11)	31.775	0.270	30.6
Fructose		t	~100	(101)	30.466	0.360	22.9
Citrate		t	72	(101)	30.223	0.412	21.4
		m	28	($\bar{1}$11)	31.808	0.304	27.2

For citrate sample, the X-ray diffraction patterns imply that although monoclinic phase has been started to form at 500 °C, a high volume fractions of zirconia has been crystallized in tetragonal form by heating at 600 and 700 °C. As Fig. 3 demonstrates, for sucrose sample, the crystallization of both monoclinic and tetragonal phases started at 500 °C and the amount of tetragonal seems to have experienced an increasing trend up to 700 °C. X-ray diffraction patterns of fructose sample calcined at different temperatures show that the tetragonal zirconia is the unique phase and there is no evidence of monoclinic phase. This can be attributed to the higher fractions of crystallization from amorphous phase for fructose sample [31]. As Table 3 shows, the sample prepared with fructose has the lowest crystallite size at 500 °C among the other ones. The crystallite size of the samples has been increased by increasing the calcination temperature [32]. Fructose sample calcined at 700 °C has also the highest crystallite size of tetragonal zirconia.

Table 4 represents the lattice parameters of tetragonal phase of fructose sample calcined at 500, 600 and 700 °C calculated from Eq. (5). In this table, *2θ* is diffraction angles, (*hkl*) is crystalline plane indices and *d* is the distance of crystalline planes. Parameters of a_c and c_c are the calculated lattice parameters of tetragonal phase (in Å) which are compared with the theoretical values of a_R (3.592(5) Å) and c_R (5.183(7) Å) as reference data obtained from the X-ray diffraction card of tetragonal zirconia phase (JCPDS-80-0965). The numbers in the parentheses show the approximate of the last digits in the calculations. These data were used for plotting Fig. 4, represent that the c_c/a_c ratio for tetragonal phase was increased by the temperature increase. According to the Table 3, the crystallite sizes were grown by increasing temperature. The strain of the tetragonal crystal lattice is caused by the applied surficial tension of the nano-scale synthesized grains and is diversely

Accepted Manuscript Not Copyedited

related to the crystallite size [33], which means that by increasing the crystallite size, it would be reduced. Hence, the *c/a* factor of unite cell would be increased and the crystals become more similar to tetragonal structure. However in lower temperatures which produce smaller crystallites, the cell structure would be under more strain, caused decreasing in *c/a* ratio. Moreover, the small observed differences between the calculated and reference crystal parameters of tetragonal phase would be related to the meta-stable structure of the synthesized powder at low temperature.

Table 4. Lattice parameters of tetragonal zirconia phase.

T / °C	(*hkl*)	2*θ* / deg.	*d* / Å	a_C / Å	c_C / Å
	[011]	30.4671	2.93407	3.589(6)	5.113(9)
500	[112]	35.2359	2.54713	3.592(2)	5.138(3)
	[110]	50.6223	1.80322	3.602(2)	5.081(9)
	[011]	30.4659	2.93417	3.575(6)	5.135(0)
600	[112]	35.3633	2.53825	3.584(4)	5.155(5)
	[110]	50.52454	1.80498	3.585(1)	5.113(9)
	[011]	30.3836	2.94193	3.561(6)	5.135(0)
700	[112]	35.3367	2.5401	3.584(4)	5.149(9)
	[110]	50.47	1.8083	3.585(1)	5.131(4)

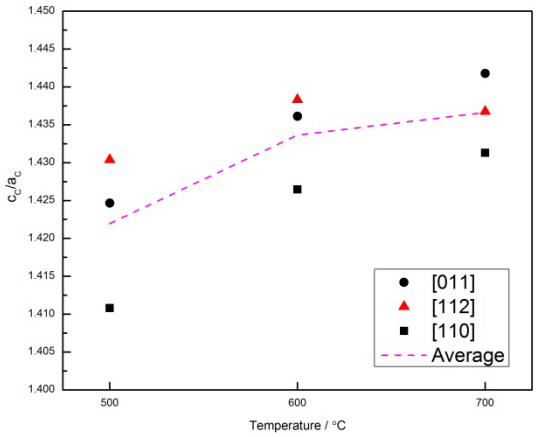

Fig. 4. Lattice parameters ratio vs. temperature.

3.3. Specific surface area/particle size

Table 5 shows the specific surface area and particle size values of synthesized nano zirconia powder using different chelating agents and calcined at 500, 600 and 700 °C for 1 h. In this table, *S* is the specific surface area and *P* is the particle

Accepted Manuscript Not Copyedited

size of the samples. As this table shows, by increasing the calcination temperature for fructose and sucrose samples, the values of specific surface area decreased and particle sizes increased. It is obvious that after calcination at 700 °C, fructose sample has the highest specific surface area (27 m^2 g^{-1}) and lowest particle size (39.12 nm) values as well. For the citrate sample, the trend is different and the highest particle size (96 nm) and lowest specific surface area (11 m^2 g^{-1}) values observed after calcination at 500 °C. By increasing the calcination temperature till 600 °C, the particles size decreased drastically and specific surface area increased. After 700 °C, the particle size and specific surface area values are again gradually increased and decreased, respectively.

Table 5. Specific surface area and particle size.

T / °C	S / m^2 g^{-1}			d / nm		
	Sucrose	Fructose	Citrate	Sucrose	Fructose	Citrate
500	86	94	11	12.3	11.2	96
600	29	35	26	36.4	30.1	40
700	21	27	23	50.3	39.1	46

In the sugar synthesis method using sucrose as a chelating agent, addition of nitric acid renders breakage of sucrose molecules into glucose and fructose, which then contributes to prevent the re-crystallization of sugar molecules. Releasing the functional groups of decomposed products leads to the bond formation between the metallic ions in a homogeneous solution, which reduces the chance of precursor precipitation [2-5]. Through the heating process, the metal ion-chelated complex is decomposed into carbon dioxide and water while a large amount of heat is generated. This phenomenon produces gases which prohibit particles agglomeration, and helps to form pores and high surface area particles [34]. Costa et al. [35] investigated the difference between the pore size distributions of the samples produced from sucrose and fructose as template materials. Their results revealed the different pore size distribution for sucrose and a homogenous one for fructose. Wide pore size range of the samples produced by sucrose allows obtaining particles with different size distribution and leads to the simultaneous formation of monoclinic and tetragonal phases [13,14,32]. This would be probably the main reason for the highest specific surface area and lowest particle size values of the fructose sample after calcination at 700 °C. According to the thermal analysis results (DTA curves of Fig. 2(A)), a strong heat released around 230 °C for citrate gel by heating. It is also clear that the zirconia formation would not be completed before 500 °C. The large crystallite size and low surface area values of citrate sample calcined at 500 °C are an evidence for such a claim. After increasing the calcination temperature till 600 °C and fulfillment of the reaction, the particle size was decreased drastically accompanied with an

Accepted Manuscript Not Copyedited

increase in specific surface area. However, by calcination at 700 °C, the particle size and specific surface area was logically increased and decreased, respectively. This observation is in agreement with the X-ray diffraction data.

3.4. Spectroscopy

Fig. 5(A) shows the Fourier transform Infra-red (FT-IR) spectra of the nano powders with different chelating agents and calcined at 700 °C. Wide observed band in the frequency range of 3100-3550 cm^{-1} and a weak band at 1640-1650 cm^{-1} are attributed to the stretching and bending vibrations of the O-H groups due to absorbed water molecules from air. Another weak vibrations appearing in the range of 2340-2360 cm^{-1} is ascribed to the coupling effect of the stretching and bending vibrations of -OH groups. The stretching of Zr-O crystalline bands shows absorption at lower frequencies. The broad absorption band and corresponding shoulder at 608-639 cm^{-1} is assigned to the Zr-O vibration of tetragonal phase. A small band in the range of 982-993 cm^{-1} is attributed to the monoclinic phase in the FTIR spectra of sucrose and citrate samples. These findings are compatible with the X-ray diffraction data. Similar observations were also reported for the FT-IR analysis of the zirconia nano particles [11,13]. Fig. 5(B) shows the Raman spectrum of the fructose based sample heated at 700 °C (A) and demonstrates the positions of the peaks of tetragonal zirconia phase. However, Raman spectroscopy characterization has the same problem as XRD technique to characterize tetragonal and cubic phases of zirconia due to giving the same patterns for them [40]. Hence, in this work, the electron diffraction using TEM was employed as the main characterization technique to validate the formation of pure tetragonal zirconia phase in the synthesized nano powder which is discussed in the next section.

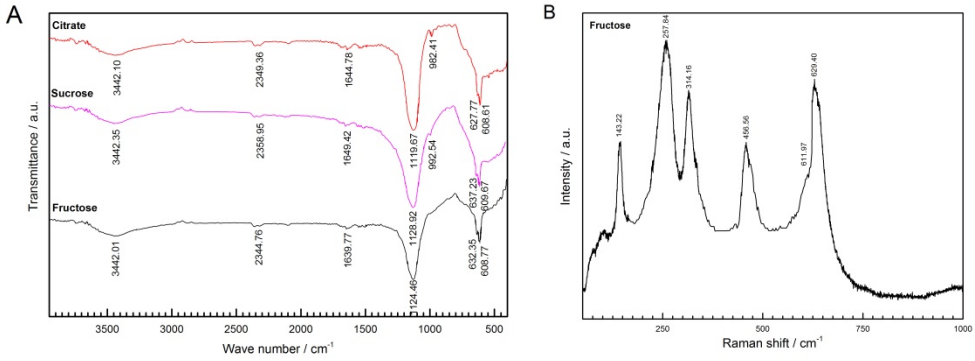

Fig. 5. FT-IR spectra of the calcined nano powders at 700 °C (A) and Raman spectrum of the heated fructose sample at 700 °C (B).

3.5. Microstructural features and morphology

Acc Manuscript Not Copyedited

Figs. 6(A) and (B) demonstrate FE-SEM micrographs and morphology of citrate sample calcined at 700 °C for 1 h. As this figure shows, the abrupt combustion of nitrate radicals and high temperature combustion of citric acid which was previously observed in the related DTA graph (Fig. 2(A)), resulted in a partially agglomeration of the synthesized particles (Fig.6 (A)) [36, 37], while the grains (Fig.6(B)) and crystallite sizes (Table 3) were remained in the nano scales. Fig. 7 indicates the morphological feature of the individual particles of sucrose sample heated at 700 °C. However, as these particles were smaller than 100 nm, the XRD pattern (Fig. 3) showed the simultaneous presence of monoclinic and tetragonal phases in this sample [9]. Electron micrographs of the sample prepared via fructose as chelating agent and fired at 700 °C are presented in Figs. 8(A) and (B). No sign of agglomeration was detected in Fig. 8(A) and pure stabilized tetragonal zirconia phase (Fig. 3) with the particle size of <40 nm (Table 5) and crystallite size of <23 nm (Table 3) was obtained after calcination at 700 °C. Fig. 8(B) illustrates the morphology of some individual synthesized tetragonal particles. For the fructose based sample heated at 700 °C, tetragonal zirconia is the only phase. As the preferable crystal growth direction of this structure is along the c axis, it is expected to result in hexagonal prisms or rod-shaped crystals in the microstructure [32]. While the growth of tetragonal zirconia phase seems to be proceeded through a uniaxial shape, the particles are not observed to have neither increased width nor an agglomerated form. In this picture, the crystal growth in the c axis direction is clear which is in agreement with the results of Fig. 4.

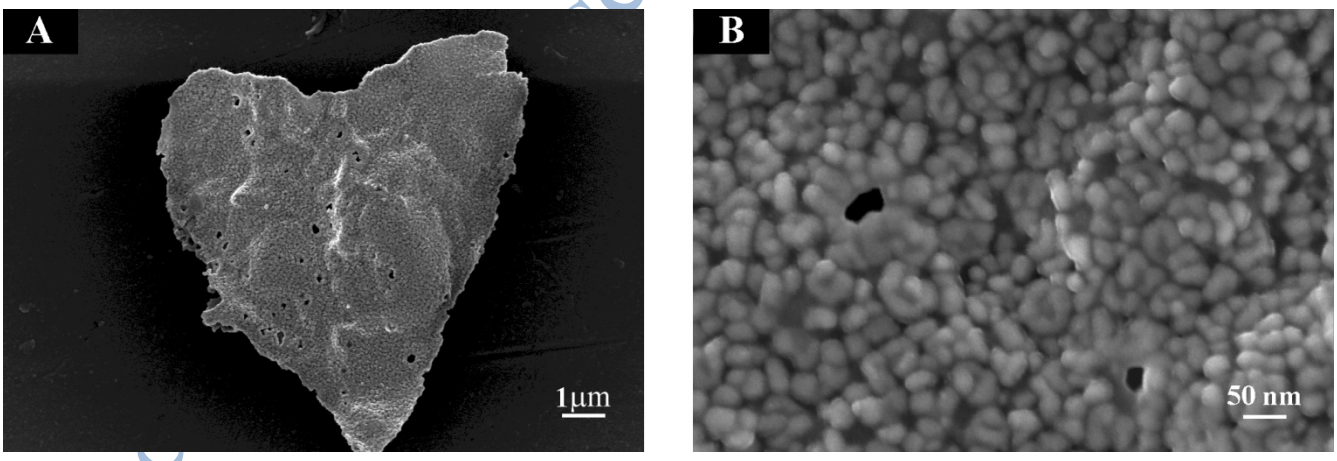

Fig. 6. SEM micrographs of citrate sample calcined at 700 °C.

Accepted Manuscript Not Copyedited

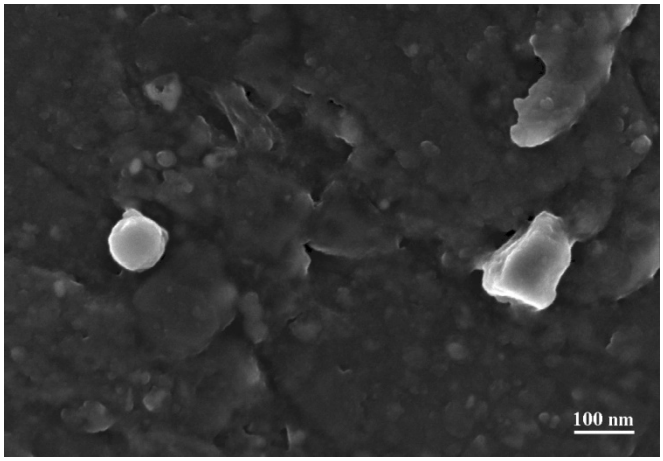

Fig. 7. SEM micrograph of sucrose sample calcined at 700 °C.

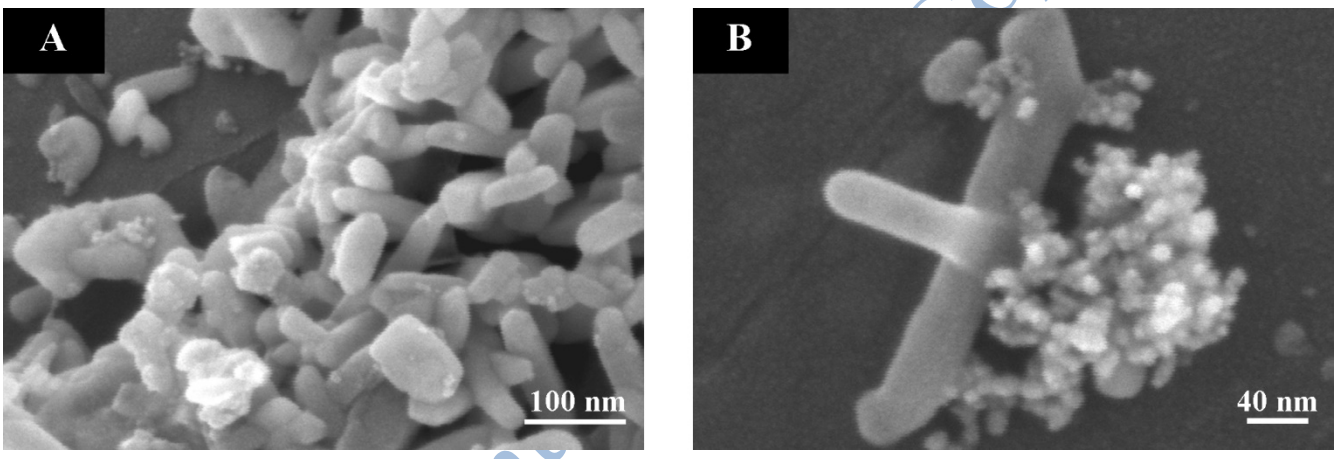

Fig. 8. SEM micrographs of fructose sample calcined at 700 °C.

Majedi et al. [38] were also investigated the green synthesis of zirconia nano particles using zirconium acetate and lemon juice and achieved cubic phase of zirconia with the particle sizes smaller than 20 nm. Ray et al. [10] have reported the production of 1, 2 and 5 mol.% Cr^{3+} doped nano-sized zirconia and investigated the phase stability by XRD. They claimed that with addition of Cr^{3+} cations, cubic zirconia would be stabilized at 600 °C. In the case of nano zirconia, the x-ray diffraction pattern of tetragonal phase becomes more similar to cubic one [3]. Small shoulder at 2θ of 59.4° (Fig. 3) is the distinguishing characteristic of tetragonal from cubic phase of zirconia. While the crystallite size of the tetragonal phase becomes smaller than 30 nm, the shoulder would locate in downgrading of the main peaks which would result in misdiagnosis of cubic phase instead of tetragonal [39,40]. The main characteristic crystallographic plane of tetragonal phase is (112) which has not been detected by X-ray diffraction (Fig. 3). In the current study, electron diffraction pattern was helpful in detection of (112) plane which is a characteristic of tetragonal zirconia phase.

Accepted Manuscript Copyedited

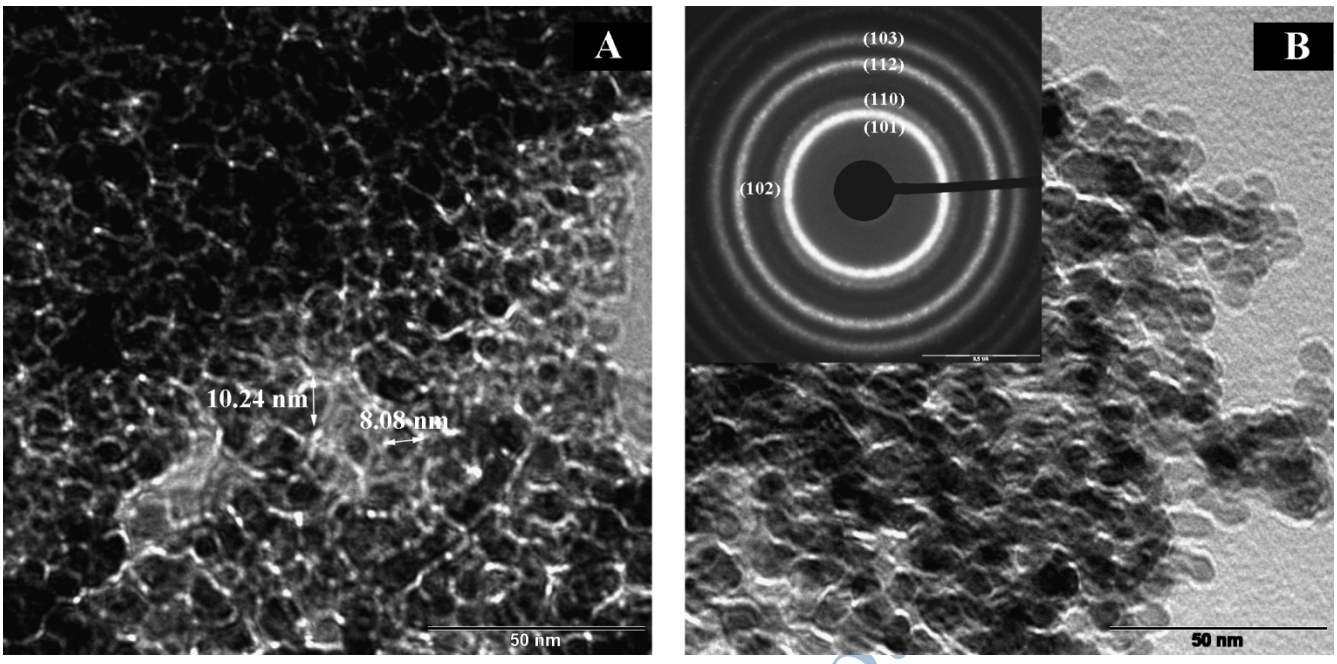

Fig. 9. Transmission electron micrograph and selected area electron diffraction (SAED) pattern of fructose sample calcined at 700 °C.

Accepted Manuscript

Figs. 9(A) and (B) represent the transmission electron micrograph and selected area electron diffraction (SAED) pattern of fructose sample fired at 700 °C. According to Fig. 9(A), the crystallite size of <9 nm is observed in this sample which is close to the calculated data from Scherrer equation (Table 3). It is possible to measure the (*hkl*) indices from electron diffraction patterns [41]. For each circle, the specific radius is calculated via the Eq. (7):

$$R\, d_{hkl} = L\, \lambda \qquad (7)$$

where, L is the camera constant (1 Å^2), *R* is the radius of circle (Å), λ is the electron beam wavelength (2.1658 Å) and d_{hkl} is the distance of planes (Å). For the (101) crystalline planes of the fructose sample, this distance was calculated to be 2.93174 Å. According to the Fig. 9(B), for the most interior circle which has the maximum of planes distances, the calculated *d* is equal to 2.93279 Å. Thus, the structure of zirconia should be tetragonal or cubic. By calculating these distances, it was concluded that these values are much closer to the values for tetragonal phase. Also, the (102) crystal plane, (which is specific of the tetragonal phase and does not present in the cubic one), is presented in this pattern. Therefore, it was determined as tetragonal phase for this sample. It can be claimed that the inset electron diffraction pattern in Fig. 9(B) indicates the existence of (102) planes and refers to the presence of tetragonal zirconia phase [29,32]. Zhang et al. [31] conducted a research on size dependency and phase stability of nano-sized zirconia. Both of their experimental results and

theoretical calculations indicated that the tetragonal zirconia crystals with of diameter (d) <14 nm are thermodynamically stable at room temperature and the crystals with 14<d<31 nm are metastable possibly due to a kinetic nucleation barrier. This barrier could prevent monoclinic phase to transform to tetragonal. As can be observed, although the crystallite size of monoclinic phase in 700 °C calcined fructose sample (Table 3) is lower than the critical diameter, this phenomenon could block the transformation of monoclinic to tetragonal phase of the synthesized zirconia particle.

4. Conclusion

In this paper the synthesis of stabilized nano tetragonal zirconia was investigated via Pechini and sugar-based methods using zirconium hydroxide, citric acid, sucrose and fructose after calcination at 500, 600 and 700 °C in air. The effects of heat treatment and chelating agents on thermal behavior, physical, phase and microstructural properties were studied. The main findings of the research can be summarized as follow:

1) According to the diffraction data, mixtures of monoclinic and tetragonal phases were observed for sucrose and citrate samples at all temperatures. In fructose sample, the tetragonal structure was the unique characterized phase. Also there was not any trace of amorphous phase in the phase composition of the samples. The crystallite sizes of tetragonal phase were determined for citrate (21.4 nm), sucrose (21.4 nm) and fructose (22.9 nm) samples after calcination at 700 °C.
2) Using BET technique, the particle sizes were measured lower than 50 nm for all samples after calcination at this temperature. These results were in agreement with the microstructural and morphological observations by electron microscopy.
3) The tetragonality of the crystal structure was also discussed by the presence of the (102) crystalline plane in the selected area electron diffraction pattern of fructose sample calcined at 700 °C. The obtained crystallite sizes from TEM micrographs (8-11 nm) was close to calculated ones from XRD and Scherrer equation (23 nm) for this sample.
4) Altogether, using fructose as chelating agents seems to be more effective to produce pure stabilized tetragonal zirconia phase at low temperature of 500 °C. Using zirconium hydroxide is also expected to make this process green and more cost-effective rather than zirconium alkoxides or salts as precursor.

Accepted Manuscript Not Copyedited

References

[1] F. Petrakli, M. Arkas, A. Tsetsekou, a-Alumina nanospheres from nano-dispersed boehmite synthesized by a wet chemical route, *J. Am. Ceram. Soc*., 103(2018), No.8, p. 3508.

[2] K. Agilandeswari, A.R. kumar, Optical, electrical properties, characterization and synthesis of $Ca_2Co_2O_5$ by sucrose assisted sol-gel combustion method, *Adv. Powder Tech*., 25(2014), No. 3, p. 904.

[3] C. Suciu, A.C. Hoffmann, A. Vik, F. Goga, Effect of calcination conditions and precursor proportions on the properties of YSZ nanoparticles obtained by modified sol-gel route, *Chem. Eng. J*., 138(2008), No. 1-3, p. 608.

[4] K. Prabhakaran, A. Melkeri, N.M. Gokhale, S.C. Sharma, Synthesis of nano crystalline 8 mol.% yttria stabilized zirconia powder from sucrose derived organic precursors, *Ceram. Int*., 33(2007), No. 8, p. 1551.

[5] Y. Wu, A. Bandyopadhyay, S. Bose, Processing of alumina and zirconia nano-powders and compacts, *Mater. Sci. Eng. A*, 380(2004), No. 1-2, p. 349.

[6] P.S. Behera, S. Bhattacharyya, R. Sarkar, Effect of citrate to nitrate ratio on the sol-gel synthesis of nanosized α-Al_2O_3 powder, *Ceram. Int*., 43(2017), No. 17, p. 15221.

[7] R.E. Juarez, D.G. Lamas, G.E. Lascalea, N.E. Walsoe de Reca, Synthesis of nano crystalline zirconia powders for TZP ceramics by a nitrate-citrate combustion route, *J. Eur. Ceram. Soc*., 20(2000), No. 2, p. 133.

[8] J. Yang, J. Lian, Q. Dong, Q. Guan, J. Chen, Z. Guo, Synthesis of YSZ nano crystalline particles via the nitrate-citrate combustion route using diester phosphate (PE) as dispersant, *Mater. Let*., 57(2003), No. 19, p. 2792.

[9] K.A. Singh, L.C. Pathak, S.K. Roy, Effect of citric acid on the synthesis of nano-crystalline yttria stabilized zirconia powders by nitrate-citrate process, *Ceram. Int.*, 33(2007), No. 8, p. 1463.

[10] J.C. Ray, P. Pramanik, S. Ram, A novel polymer matrix method for synthesizing ZrO_2 nanocrystals at moderate temperature, *J. Mater. Sci. Let*., 20(2001), No. 22, p. 2017.

[11] A. Majedi, F. Davar, A. Abbasi, Sucrose-mediated sol-gel synthesis of nano sized pure and S-doped zirconia and its catalytic activity for the synthesis of acetyl salicylic acid, *J. Ind. Eng. Chem*., 20(2014), No. 6, p. 4215,.

[12] H. Zhu, B. Liu, M. Shen, Y. Kong, X. Hong, Y. Hu, W. Ding, L. Dong, Y. Chen, Effect of maltose for the crystallization of tetragonal zirconia, *Mater. Let*., 58(2004), No. 25, p. 3107.

[13] F. Heshmatpour, R.B. Aghakhanpour, Synthesis and characterization of nano crystalline zirconia powder by simple sol-gel method with glucose and fructose as organic additives, *Powder Tech*., 205(2011), No. 1-3, p. 193.

[14] R.D. Purohit, S. Saha, A.K. Tyagi, Combustion synthesis of nano crystalline ZrO_2 powder: XRD, Raman spectroscopy and TEM studies, *Mater. Sci. Eng. B*, 130(2006), No. 1-3, p. 57.

Accepted Manuscript Not Copyedited

[15] M.M. Rashad, H.M. Baioumy, Effect of thermal treatment on the crystal structure and morphology of zirconia nano powders produced by three different routes, *J. Mater. Proc. Tech*., 195(2008), No. 1-3, p. 178.

[16] F. Maglia, M. Dapiaggi, I. Tredici, B. Maroni, U. Anselmi-Tamburini, Synthesis of fully dense nanostabilized undoped tetragonal zirconia, J. *Am. Ceram. Soc*., 93(2010), No. 7, p. 2092.

[17] F. Davar, A. Hassankhani, M.R. Loghman Estarki, Controllable synthesis of metastable tetragonal zirconia nano crystals using citric acid assisted sol-gel method, *Ceram. Int*., 39(2013), No. 3, p. 2933.

[18] V.V. Srdic, M. Winterer, H. Hahn, Sintering behavior of nano crystalline zirconia prepared by chemical vapor synthesis, *J. Am. Ceram. Soc*., 83(2000), No. 4, p. 729.

[19] N. Nafsin, H. Li, E.W. Leib, T. Vossmeyer, P. Stroeve, R.H.R. Castro, Stability of rare earth doped spherical yttria stabilized zirconia synthesized by ultrasonic spray pyrolysis, *J. Am. Ceram. Soc*., 100(2017), No. 10, p. 4425.

[20] J. Joo, T. Yu, Y.W. Kim, H.M. Park, F. Wu, J.Z. Zhang, T. Hyeon, Multigram scale synthesis and characterization of monodisperse tetragonal zirconia nano crystals, *J. Am. Chem. Soc*., 125(2003), No. 21, p. 6553.

[21] N. Chandra, D.K. Singh, M. Sharma, R.K. Upadhyay, S.S. Amritphale, S.K. Sanghi, Synthesis and characterization of nano-sized zirconia powder synthesized by single emulsion-assisted direct precipitation, *J. Colloid Interface Sci*., 342(2010), No. 2, p. 327.

[22] U.K.H. Bangi, C.S. Park, S. Baek, H.H. Park, Sol-gel synthesis of high surface area nanostructured zirconia powder by surface chemical modification, *Powder Tech*., 239(2013), No. 5, p. 314.

[23] S. Shukla, S. Seal, R. Vij, S. Bandyopadhyay, Effect of HPC and water concentration on the evolution of size, aggregation and crystallization of sol-gel nano zirconia, *J. Nano Particle Res*., 4(2002), No. 6, p. 553.

[24] C. Suchomski, D.J. Weber, P. Dolcet, A. Hofmann, P. Voepel, J. Yue, M. Einert, M. Moller, S. Werner, S. Gross, I. Djerdj, T. Brezesinski, B.M. Smarsly, Sustainable and surfactant-free high-throughput synthesis of highly dispersible zirconia nano crystals, *J. Mater. Chem. A*, 5(2017), No. 31, p. 16296.

[25] F. Kazemi, S. Sohrabi, S. Malek-Ahmadi, H.R. Rezaie, S.R. Allahkaram, Synthesis of metastable tetragonal zirconia nano powder during extraction of zirconia from zircon by alkaline fusion process, [in] *The International Conference on Ultrafine Grained and Nanostructured Materials*, Tehran, Iran, 2007, p.75.

[26] R. Jenkins, R. Snyder, *Introduction to X-Ray Powder Diffractometery*, 2nd edition, John Wiley & Sons, USA, 2012, p. 25.

[27] A. Saberi, B. Alinejad, Z. Negahdari, F. Kazemi, A. Almasi, A novel method to low temperature synthesis of nanocrystalline forsterite, *Mat. Res. Bul*., 42(2007), No. 4, p. 666.

Accepted Manuscript Not Copyedited

[28] R. Naghizadeh, F. Kazemi, F. Arianpour, R. Ghaderi, M. Haj Fathalian, M. Taheri, H.R. Rezaie, A novel method for quantitative phase determination of cristobalite in ceramic cores using differential scanning calorimeter, *J. Thermal Analysis Calorimetry*, 119(2014), No. 1, p. 191.

[29] K.A. Aly, N.M. Khalil, Y. Algamal, Q.M.A. Saleem, Estimation of lattice strain for zirconia nano-particles based on Williamson- Hall analysis, *Mat. Chem. Phys*., 193(2017), No. 6, p. 182.

[30] C.J. Szepesi, J.H. Adair, High yield hydrothermal synthesis of nano-scale zirconia and YTZP, *J. Am. Ceram. Soc*., 94(2011), No. 12, p. 4239.

[31] Y.L. Zhang, X.J. Jin, Y.H. Rong, T.Y. Hsu, D.Y. Jiang, J.L. Shi, The size dependence of structural stability in nano-sized ZrO_2 particles, *Mater. Sci. Eng. A*, 438-440(2006), No. 25, p. 399.

[32] F. Kazemi, A. Saberi, S. Malek-Ahmadi, S. Sohrabi, H.R. Rezaie, M. Tahriri, A novel method for synthesis of metastable tetragonal zirconia nano powders at low temperatures, *Ceram. Silikaty*, 55(2011), No. 1, p. 26.

[33] C.C. Koch, Nanostructured Materials, Processing, Properties and Potential Applications, William Andrew, New York, 2002, p. 4.

[34] R.N. Das, A. Bandyopadhyay, S. Bose, Nano crystalline alpha Al_2O_3 using sucrose, *J. Am. Ceram. Soc*., 84(2001), No. 10, p. 2421.

[35] J.C. Diniz da Costa, S. Coombs, Characterization of xerogels derived from sucrose template sol-gel synthesis, *J. Sol Gel Sci. Tech.*, 31(2004), No. 1-3, p. 215.

[36] R. Mahendran, S.P. Kumaresh Babu, S. Natarajan, S. Manivannan, A. Vallimanalan, Phase transformation and crystal growth behavior of 8mol% ($SmO_{1.5}$, $GdO_{1.5}$, and $YO_{1.5}$) stabilized ZrO_2 powders, Int. J. Miner. Metall. Mater. 24(2017), No. 7, P. 842.

[37] A. Srivastava, M.K. Dongare, Low-temperature preparation of tetragonal zirconia, Mater. Let., 5(1987), No. 3, p. 111.

[38] A. Majedi, A. Abbasi, F. Davar, Green synthesis of zirconia nanoparticles using the modified Pechini method and characterization of its optical and electrical properties, J. Sol Gel Sci. Technol., 77(2016), No. 3, p. 542.

[39] E. Djurado1, E. Meunier, Synthesis of doped and un-doped nano powders of tetragonal polycrystalline zirconia (TPZ) by spray-pyrolysis, J. Solid State Chem., 141(1998), No. 1, p. 191.

[40] A. Bumajdad, A.A. Nazeer, F.A.l Sagheer, S. Nahar, M.I. Zaki, Controlled synthesis of ZrO_2 nanoparticles with tailored size, morphology and crystal phases via organic/inorganic hybrid films, Scientific Reports, 8(2018), No. 3695, p. 1.

Accepted Manuscript Not Copyedited

[41] X. Zou, S. Hovmoller, P. Oleynikov, Electron Crystallography: Electron Microscopy and Electron Diffraction, Oxford University Press, 1st Edition, 2011, p, 98.

Accepted Manuscript Not Copyedited